Formation of nano-oriented crystals of iPP with ultrahigh performance crystallized by extreme melt elongation

String- or chain-like molecules can form complex structures; they perform multiple functions and can carry information. As we can see with most natural materials such as DNA and proteins, many sophisticated materials have developed over several billion years. However, in the case of polymers, it is impossible to obtain ideal crystals with ultimate performance of function, because "entanglements" of molecular chains suppress structure formation and the expression of function. For example, polymer chains are conventionally ordered from isotropic melts during "crystallization." However, this ordering is difficult, since it is not easy for entangled chains to slide along their chain axes and disentangle into an ordered parallel arrangement. Therefore, amorphous areas remain in the solid. As conventional polymer solids are composed of amorphous and crystal parts, their crystallinity is much less than unity [1]. Such polymer solids show poor performance, as the amorphous portion takes the structure of a frozen melt.

Crystallization is a well-known ordering process from the melt or a gas. The structures and physical properties depend on crystallization conditions. If we could control the entanglements of polymer chains by crystallization, we would obtain a material with excellent performance and/or function.

The polymer chain in the melt or a solution changes its shape under an external field, such as elongation and shear. If we could induce significant elongation to the melt, the elongation should affect the bulky melt and the crystallization behavior and properties of polymer solids should significantly change. Hereafter, we will name the crystallization under melt elongation as "elongational (melt) crystallization." However, the significant elongational crystallization has been difficult.

We succeeded in realizing an extreme melt elongation for the first time by developing a "compression method" [2]. Figure 1(a) shows the principle of the compression method. We compressed the supercooled melt by sandwiching it between two plates. By this method, the melt was stretched along a direction perpendicular to the compressed direction. Figure 1(b) shows a roll-type apparatus.

The purposes of this work are to show the formation of nano-oriented crystals (NOCs) with ultrahigh performance by elongational crystallization under an extreme elongational field and to clarify the structure and nucleation mechanism of NOCs.

We used isotactic polypropylene (iPP, M_w=34×10^4, M_w/M_n=30) as a model polymer, where M_w is the weight-average molecular weight and M_w/M_n is

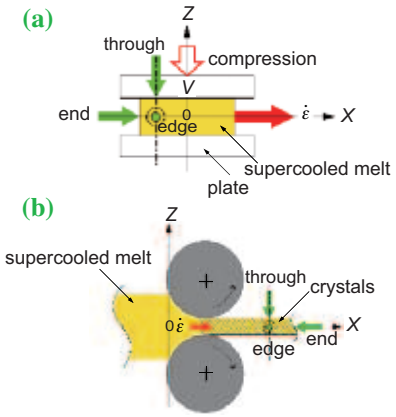

Fig. 1. Schematic illustration of principle of elongational crystallization by compression method. The *Z*-axis is along the direction of compression and the *X*-axis is parallel to the elongational direction. **(a)** Compression-type apparatus. Both 1D and 2D compression-type crystallizations are applicable. **(b)** Roll-type apparatus. It is 1D compression-type crystallization.

the index of dispersion. The equilibrium melting temperature (T_m^0) in a quiescent field was 187°C [3]. The sample was melted at above T_m^0, cooled to the crystallization temperature (T_c = 150°C) and then compressed to elongate the supercooled melt into a sheet or plate. The former is one-dimensional (1D) compression-type crystallization and the latter is two-dimensional (2D) compression-type crystallization. Small/wide angle X-ray scattering (SAXS/WAXS) observation was carried out at **BL03XU** and **BL40B2**.

Figures 2(a) and 2(c) and 2(b) and 2(d) show typical SAXS and WAXS patterns for small and large elongational strain rates ($\dot{\varepsilon}$), respectively. Figures 2(a) and 2(c) for small $\dot{\varepsilon}$ mainly showed well-known unoriented long-period patterns (L1 and L2) and a

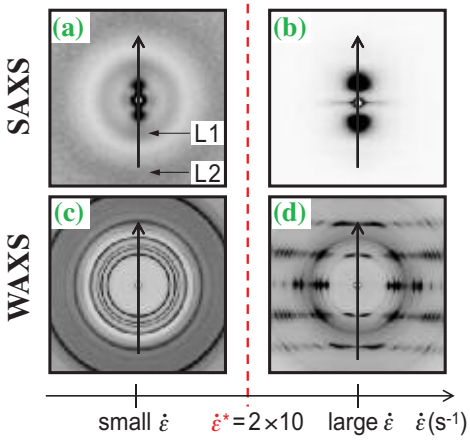

Fig. 2. $\dot{\varepsilon}$ dependence of scattering patterns for through-view. Samples were crystallized by 1D compression. Meridian arrows show the elongational direction. **(a)** SAXS pattern of small $\dot{\varepsilon}$. **(b)** WAXS pattern of small $\dot{\varepsilon}$. **(c)** SAXS pattern of large $\dot{\varepsilon}$. **(d)** WAXS pattern of large $\dot{\varepsilon}$.

Debye-Scherrer ring pattern, respectively. Therefore, the dominant structure was the conventional stacked lamellar structure. Figures 2(b) and 2(d) for large $\dot{\varepsilon}$ showed an oriented two-point pattern and a highly oriented fiber pattern along the melt-elongational direction, respectively. Since the NOCs showed a high crystallinity of about unity, the oriented two-point pattern means that the crystals are randomly oriented, such as 1D paracrystals or a 1D liquid-like packing of particles [4]. From the structural analysis of the SAXS and WAXS patterns, the structure model of the NOCs was obtained (Fig. 3(b)). Nanocrystals with sizes of 20-30 nm were linked and oriented along the elongational direction. Stems were also oriented along the elongational direction. Thus, the scattering pattern discontinuously changed at a critical $\dot{\varepsilon}$ ($\dot{\varepsilon}^*$).

$\dot{\varepsilon}^* = 2\times10^2$ s^{-1} was obtained from the NOC fraction f(NOCs) within the crystalline volume. Figure 4 shows f(NOCs) agains $\dot{\varepsilon}$, which was obtained by analyzing WAXS intensity. The basic viewpoint of this analysis is as follows: As the WAXS patterns of the NOCs and unoriented crystals show typical fiber and Debye-Scherrer patterns, respectively, these regions are well-known in the X-ray scattering theory [5]. When the NOCs and unoriented crystals are mixed, the scattering intensity (I_X) from the (hkl) reflection of NOCs can be estimated by subtracting the I_X of unoriented crystals from the observed I_X. With an increase in $\dot{\varepsilon}$, f(NOCs) increases slightly, then significantly at $\dot{\varepsilon} \cong 10^2$ s^{-1}, and finally saturates. We defined $\dot{\varepsilon}^*$ as $\dot{\varepsilon}$, where f(NOCs) becomes 0.6.

Figure 3 shows a schematic illustration of the nucleation mechanism and the structure model of the NOCs. Figure 3(a) is illustrated by focusing on one random coil of one polymer chain within the bulky melt. Polymer chains should be elongated along the elongational direction when the melt is compressed with a large $\dot{\varepsilon}$. Many parallel packings of chains would be generated, and an infinite number of nuclei would be formed. Then, they grow instantaneously into nanocrystals before the melt structure randomizes by entropic relaxation. During the growth, entanglements should be condensed to the interface between the nanocrystals (Fig. 3(b)). One chain should three-dimensionally interpenetrate and connect the nanocrystals more than 10^2 times, as the mean extended length of one polymer chain is about 2 μm. This model was called the "YOROI" model, as its structure is similar to the armor of samurai in ancient Japan.

The NOCs showed an ultrahigh performance: the tensile strength at break was about 2.3×10^2 MPa, which was comparable to that of metals, Young's modulus was 4.1 GPa. The thermal resistance was 176°C. The origin of these performance characteristics of the NOCs can be explained by the YOROI model. NOCs will be useful in a wide variety of applications and will contribute to the effort to construct a sustainable society by enabling the development of lightweight devices.

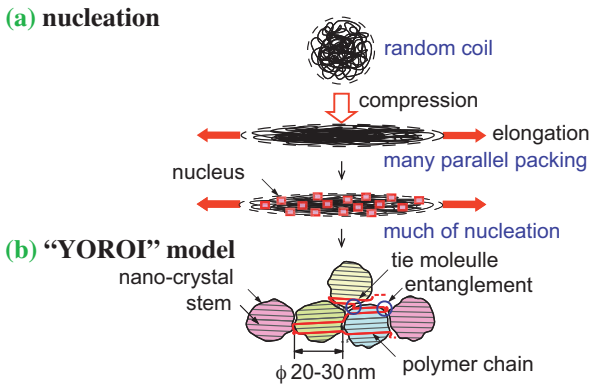

Fig. 3. Schematic illustration of crystallization of NOCs. **(a)** Nucleation mechanism of NOCs. **(b)** YOROI model of the NOC structure.

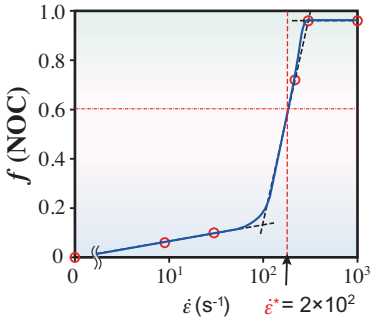

Fig. 4. f(NOCs) against $\dot{\varepsilon}$ including 1D and 2D compression-type crystallizations.

Kiyoka N. Okada and Masamichi Hikosaka*

Graduate School of Integrated Arts and Sciences, Hiroshima University

*E-mail: hikosaka@hiroshima-u.ac.jp

References

[1] E.P. Moore: Polypropylene handbook Ch.3 (Kogyo Chosakai, Tokyo, 1998).
[2] *K.N. Okada, J. Washiyama, K. Watanabe, S. Sasaki, H. Masunaga and M. Hikosaka: Polymer J.* ***42*** *(2010) 464.*
[3] K. Yamada *et al.*: J. Macromol. Sci. Phys. B **42** (2003) 733.
[4] A. Guinier: Theorie et technique de la radiocristallographie Ch.10-11 (Dunod, Paris, 1964).
[5] I. Nitta: X-sen kessyougaku, the first volume 117-121 (Maruzen, Tokyo, 1959). (in Japanese)